scientific reports

Check for updates

OPEN

Pore scale insights into salinity driven foam stability and conformance control in heterogeneous porous media

Amir Hossein Molaei, Matin Shahin & Mohammad Simjoo✉

The potential application of foam for conformance control in heterogeneous reservoirs is critically dependent on brine salinity, yet the underlying pore-scale mechanisms involving residual oil have remained unclear. This study provides a pore-scale analysis, using a two-layer heterogeneous micromodel, to unravel how salinity (5,000 vs. 35,000 ppm NaCl) governs the complex interplay between foam and in-situ generated emulsions using sodium dodecyl sulfate (SDS) surfactant. In the absence of oil, low-salinity conditions produced a homogeneous, fine-textured SDS foam with high stability, leading to improved sweep efficiency across both high- and low-permeability layers. High salinity, by compressing the electrical double layer, yielded a coarse, heterogeneous foam with reduced stability due to enhanced coalescence and Ostwald ripening. The presence of residual oil revealed a critical paradigm shift: ultimate performance is not dictated by foam stability alone. At high salinity, the formation of coarse, unstable oil-in-water emulsion droplets, a consequence of ionic shielding, proved decisive. These large droplets acted as dynamic diverting agents, synergizing with foam to create temporary blockages in high-permeability pore throats via the Jamin effect. This mechanism effectively diverted flow into the low-permeability zone, significantly improving conformance. In contrast, the fine, stable emulsions formed at low salinity failed to block high-permeability pathways and instead caused unintended blockages within the low-permeability layer itself. Consequently, high-salinity foam injection achieved a final oil recovery of 88.02%, a significant 9.20-percentage-point improvement over the 78.81% recovery at low salinity. These results provided the first direct pore-scale evidence that optimizing salinity can tune the balance between foam stability and in-situ emulsion generation to maximize conformance control. This insight is crucial for designing effective foam strategies for enhanced oil recovery and also gas-based storage in saline, heterogeneous formations.

Keywords Salinity, Foam, Layered micromodel, Mobility, Conformance control, Emulsion

Sandstone oil reservoirs are recognized as a strategic subsurface energy resource in the global oil market and are found in various regions worldwide[1]. These reservoirs often contain significant amounts of residual oil after primary extraction, necessitating the use of enhanced oil recovery (EOR) techniques. Methods such as gas or chemical injection are frequently employed to extract the remaining oil, significantly improving recovery efficiency[2–6]. However, a major challenge in sandstone reservoirs is reservoir heterogeneity, which can substantially impact the effectiveness of oil recovery processes[7,8]. During oil production, the presence of high-permeability zones in the sandstone reservoir often leads to water channeling, reducing volumetric sweep efficiency. This issue results in non-uniform fluid distribution within the reservoir, adversely affecting extraction efficiency[9–11].

The term of reservoir conformance refers to the degree to which the injected fluid can uniformly displace hydrocarbons across the reservoir and direct them toward the production well[12]. Thus, conformance control encompasses any technique designed to enhance hydrocarbon movement from the reservoir to the production well, particularly in areas where fluid flow is more challenging. Minimizing water production is a crucial step in improving oil recovery efficiency, as excessive and premature water production not only shortens the well's productive lifespan but also increases the cost of handling produced water[13,14]. This issue presents a significant

Faculty of Petroleum and Natural Gas Engineering, Sahand University of Technology, Tabriz, Iran. ✉email: Simjoo@sut.ac.ir

economic challenge for oil companies. Controlling excessive water and gas production can enhance profitability by preventing the bypassing of oil due to injected fluids[15]. To address these challenges, different methods for controlling conformance in oil reservoirs have been introduced[16–18]. Among them, one of the most effective techniques for improving conformance in oil reservoirs is surfactant-based foam injection, which is recognized as a promising method in improving oil recovery (IOR) processes[19–21]. The main advantage of foam over other injection methods is its ability to foam the gas in situ, which can overcome the challenges associated with gas-based injection methods[22,23]. Foam injection can provide high potential to enhance macroscopic sweep efficiency and microscopic displacement efficiency by increasing effective viscosity, blocking high-permeability zones, redirecting fluid flow, and reducing capillary forces due to surfactant presence[24–26]. In high-permeability layers, foam can exhibit reduced mobility, effectively restricting flow in these zones and directing it towards low-permeability regions. Despite its advantages, foam stability in reservoir conditions remains a critical challenge in utilizing foam for conformance control[27]. Factors such as oil presence and high salinity can destabilize the foam structure[20,28]. Foam stability is essential for successful conformance control, as it determines the effectiveness of foam in blocking unwanted fluid flow in porous media[29,30].

The presence of salt ions in brine reduces the interfacial potential between the liquid and gas phases, weakening the repulsive forces between foam layers. This promotes film thinning and accelerates liquid drainage, ultimately leading to foam destabilization[31]. The ionic interactions between foaming agents and salt can have varying effects on foam stability, either enhancing or reducing its stability[32]. Additionally, the presence of oil in porous media negatively affects foam stability by decreasing the ability of the surfactant solution to generate stable foam[33]. Thus, understanding foam flow dynamics in porous media is crucial for the success of advanced oil recovery techniques and effective conformance control[34]. Core flooding experiments are commonly used to provide macroscopic information of foam flow, such as pressure variations and gas/liquid saturation profiles. However, the geometric complexity of core samples makes direct observation of foam flow at the microscopic scale challenging. Imaging techniques such as computed tomography scanning and nuclear magnetic resonance spectroscopy have been utilized[35,36], but these methods generally lack the ability to provide high-resolution dynamic images to address the pore-scale events[37]. In this context, micromodels serve as a powerful tool for a more detailed investigation of conformance control mechanisms and also water blockage at the microscale[34]. The use of micromodels in this study aims to provide mechanistic insights into the foam flow behavior within porous media. Several studies have explored foam flow behavior for conformance control and oil production enhancement. Multiple field trials using CO_2-generated foam for conformance control have been successfully conducted. For example, the foam pilot implemented in the Salt Creek field in Wyoming demonstrated that foam injection resulted in over 25,000 barrels of additional oil recovery and a 22% reduction in gas injection requirements[38]. Similarly, successful field trials in heterogeneous carbonate reservoirs in West Texas have shown significant improvements in conformance control[39]. Another field trial conducted in the Cupiagua oil field in Colombia yielded positive results in terms of pressure maintenance and oil production enhancement[40]. Laboratory investigations have shown that foam can effectively block high-permeability zones, redirecting fluid flow toward low-permeability regions, thereby improving microscopic displacement efficiency[41]. Wang et al. conducted experiments in sandpacks and micromodels, revealing that uniform, dense, and fine-textured foam exhibited stronger blocking capabilities[42]. However, Friedman and Jensen demonstrated that oil saturation exceeding 20% significantly reduces foam stability[43]. Bello et al. reported foam stability using sodium alpha-olefin sulfonate surfactant at different salinity levels. The results indicated that foam stability increases only at low salinity, while foam stability decreases when the salt concentration exceeds a certain value[44]. Le et al. investigated foam stability under dynamic conditions with sodium chloride salinity ranging from 5% to 25% by weight. In this study, Atomeen was used as the foaming agent. Their findings showed that the resulting foam exhibited better stability at higher salinity levels[45]. Although high salinity generally reduces foam stability, in some cases, ionic interactions between foaming agents and salt can influence foam stability under high-salinity conditions. While elevated salinity typically diminishes foam stability, specific ionic interactions between surfactants and salts may enhance foam performance under high-salinity environments.

While the previously reported field and laboratory studies highlighted the potential applications of foam for conformance control, they also underscore the need for a deeper understanding of the factors that limit foam effectiveness under varying reservoir conditions. Despite the significant progress made in understanding foam behavior for conformance control, critical gaps remain regarding the influence of heterogeneity, salinity, and residual oil on foam stability and its flow dynamics. Addressing these gaps, the present study aims to provide a mechanistic insight into foam performance within a two-layer heterogeneous micromodel system that allows for cross-flow between layers. This setup aims to mimic realistic reservoir conditions with distinct permeability contrasts, enabling a detailed investigation of foam's ability to redirect injected fluids from high-permeability zones to low-permeability regions. To assess the combined effects of salinity and residual oil on foam stability, foam injection experiments were conducted at salinity levels of 5,000 ppm and 35,000 ppm both in the absence and presence of waterflooded residual oil. The experimental data, complemented by microscopic flow visualization, provided an in-depth understanding of the key mechanisms influencing conformance control by foam in a two-layer heterogeneous system.

Materials and methods

Design of a dual-layer micromodel with permeability contrast

A heterogeneous two-layer micromodel with a permeability contrast (a two-fold difference) and hydraulic connectivity was designed to accurately investigate the dominant flow mechanisms during foam injection process. As depicted in Fig. 1, the micromodel structure consists of a heterogeneous dual-layer system with precise dimensions: 3.2 cm in height, 8.12 cm in length, and a channel depth of 0.02 cm, exhibiting an overall

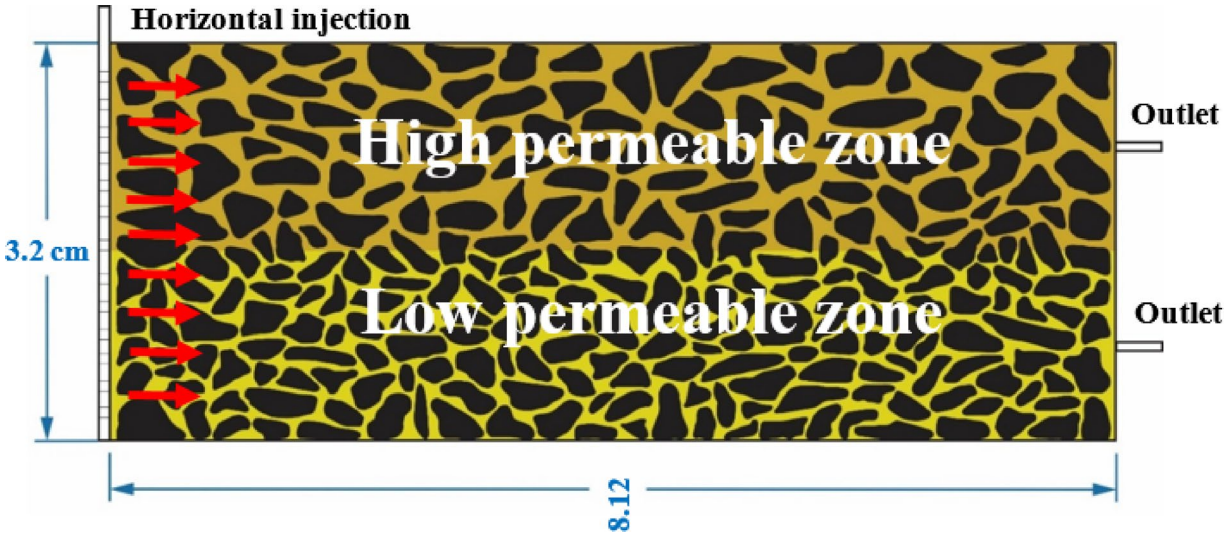

Fig. 1. Schematic representation of the designed micromodel used in this study.

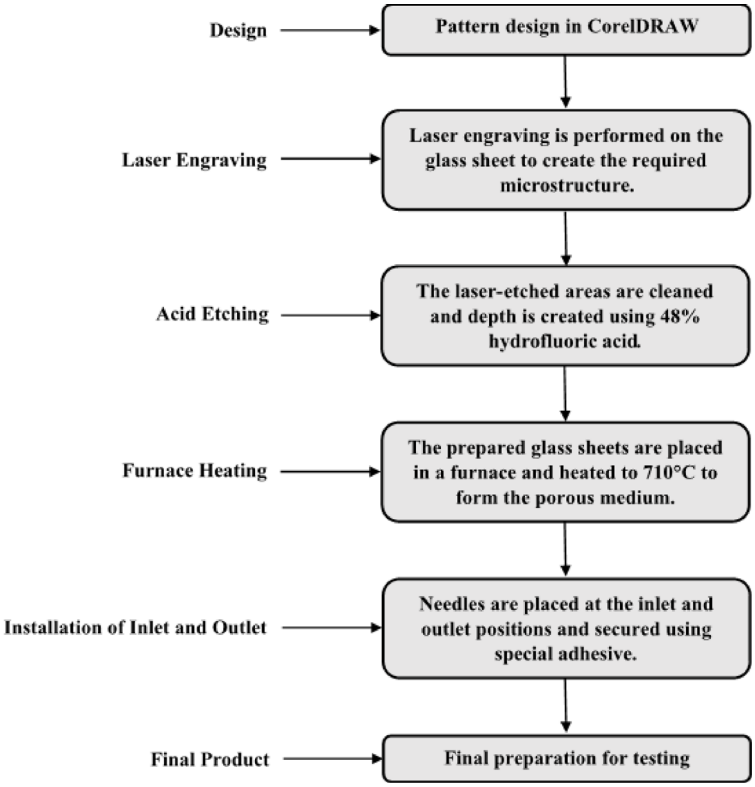

Fig. 2. Schematic diagram of the fabrication process for the designed micromodel.

porosity of approximately 48%. The entire fabrication process, illustrated in Fig. 2, was meticulously followed to ensure consistency, minimize experimental variability, and enhance the reproducibility of results.

Materials and procedures

In this study, the foaming agent solution of sodium dodecyl sulfate (SDS) at the concentration of 0.33 wt% was prepared in brine with salinity of 35,000 ppm and 5,000 ppm sodium chloride. To facilitate micromodel imaging, brine solution and kerosene (the oil phase) were dyed using methylene blue and Sudan red, respectively. Air was used as the gas phase throughout the experiments. To ensure that the dyes did not affect the behavior of the foam agent, preliminary tests such as surface tension measurements were conducted. Also, each micromodel experiment was performed once under identical operating conditions.

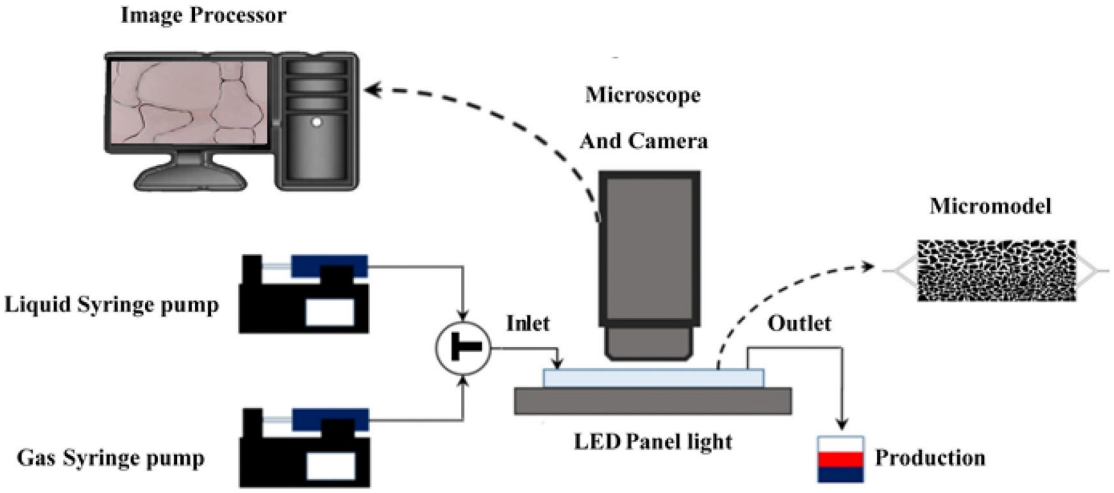

Fig. 3. Schematic of the micromodel setup used in this study.

Test no.	Experiment description	Initial condition	Salinity	Experiment procedure				
1	Absence of oil	Water saturated	35,000 ppm	Co-injection of SDS at 0.002 mL/min and gas at 0.006 mL/min	-	-	-	-
2		Water saturated	5,000 ppm	Co-injection of SDS at 0.002 mL/min and gas at 0.006 mL/min	-	-	-	-
3	Absence of oil	SDS saturated	35,000 ppm	Co-injection of SDS at 0.002 mL/min and gas at 0.006 mL/min	-	-	-	-
4		SDS saturated	5,000 ppm	Co-injection of SDS at 0.002 mL/min and gas at 0.006 mL/min	-	-	-	-
5	Presence of oil	Waterflooded residual oil	35,000 ppm	Oil injection at 0.2 mL/min	Water Injection at 0.002 mL/min	Water Injection at 0.02 mL/min	SDS Injection at 0.002 mL/min	Co-injection of SDS at 0.002 mL/min and gas at 0.006 mL/min
6		Waterflooded residual oil	5,000 ppm	Oil Injection at 0.2 mL/min	Water Injection at 0.002 mL/min	Water Injection at 0.02 mL/min	SDS Injection at 0.002 mL/min	Co-injection of SDS at 0.002 mL/min and gas at 0.006 mL/min

Table 1. Summary of all experiments performed in this study to investigate foam performance for conformance control.

The schematic of the experimental setup is shown in Fig. 3. This setup was designed to investigate the simultaneous injection of gas and foaming agent in a two-layered micromodel. In this setup, two syringe pumps were used for fluid injection: one for injecting liquid phase and the other for injecting gas phase. These two fluids were mixed through a T-shaped connector before entering the micromodel. To accurately capture the flow process and fluid saturation distribution within the micromodel, a uniform light source was placed beneath the micromodel. This uniform illumination enhances image contrast and improves the accuracy of image processing. A fixed digital camera was positioned above the model to automatically capture images at predetermined time intervals. These images were then transferred to a computer, where they were analyzed using image processing techniques. In addition to counting foam bubbles, oil recovery was also quantified from the captured images using ImageJ software.

Experimental design

In this study, micromodel experiments were conducted under ambient conditions within a horizontal flow system. The objective of these experiments was to investigate the performance of foam flow for conformance control and to evaluate the role of cross-flow in a two-layered heterogeneous system. To achieve this goal, six injection scenarios were designed in which foam with a constant quality was injected in the presence or absence of waterflooded residual oil and at different salinity levels. Table 1 gives a summary of all experiments performed in this study. The first two experiments were defined as the baseline, in which gas and surfactant solution were co-injected without any prior surfactant injection (no surfactant preflush). These scenarios were carried out in the absence of oil, under two different salinity levels (35,000 ppm and 5,000 ppm), to evaluate the foam flow behavior without surfactant preflush. The remaining four experiments involved surfactant preflush prior to foam injection. These scenarios were also conducted both with and without waterflooded residual oil, and at the salinity of 5,000 and 35,000 ppm. It is noteworthy that in all oil-present experiments, the inlet region of the micromodel was considered oil-free and was used as the in-situ foam generator chamber.

Results

Foam injection into water-saturated heterogeneous porous media

In this section, the behavior of foam flow in a water-saturated porous media was investigated using a two-layer heterogeneous micromodel at two salinity levels (5,000 and 35,000 ppm). Foam injection was performed by simultaneously injecting SDS solution and air, and micromodel images were captured at different time intervals (4, 8, 12, 24 min, and the final time) (Fig. 4). At 35,000 ppm salinity (Fig. 4, a to e), the SDS-stabilized foam tends to advance through the high-permeability layer after 4 min. However, the foam bubbles formed at this salinity were mostly large and uneven, merging quickly. This phenomenon, caused by the bursting of thin foam films (lamellae) and bubble coalescence, led to foam instability. Accordingly, the SDS-stabilized foam at 35,000 ppm salinity was unable to control the gas front effectively, and the gas and surfactant solution moved almost separately through the porous medium, without forming an efficient foam for flow control. After 8 min, the weak foam primarily traversed the high-permeability layer and failed to divert into the low-permeability layer. This trend continued until 12 min, leaving the low-permeability layer almost untouched. However, after 24 min, the SDS foam became further stabilized in particular near the inlet section and then moved into both layers. At the end of the test (final time), the SDS foam covered the entire of micromodel, but due to its initial low stability, weak conformance between the two layers was observed. At 5,000 ppm salinity (Fig. 4, f to j), the SDS foam started advancing through the high-permeability layer after 4 min. In contrast to the higher salinity, it demonstrated better stability from the outset. By 8 min, the SDS foam advanced simultaneously in both high-permeability and low-permeability layers, indicating improved conformance control. After 12 min, the advancing foam front showed more advancement in high permeable layer, but it still directed fluid flow toward low permeable layer as well. After 24 min, the SDS foam provided better conformance, and by the final time, it covered the entire of the micromodel. These results demonstrated that at lower salinity, the SDS foam exhibited better and more uniform fluid distribution.

The above results indicated that salinity plays a significant role in foam stability and its performance in conformance control. At 35,000 ppm salinity, the high salt concentration reduced the surface potential at the gas-liquid interface, which weakened the repulsive forces between foam lamellae and, consequently, decreased foam stability. In contrast, at 5,000 ppm salinity, the salt concentration was not high enough to severely affect foam stability. This allowed the foam to remain more stable from the beginning and to more effectively direct

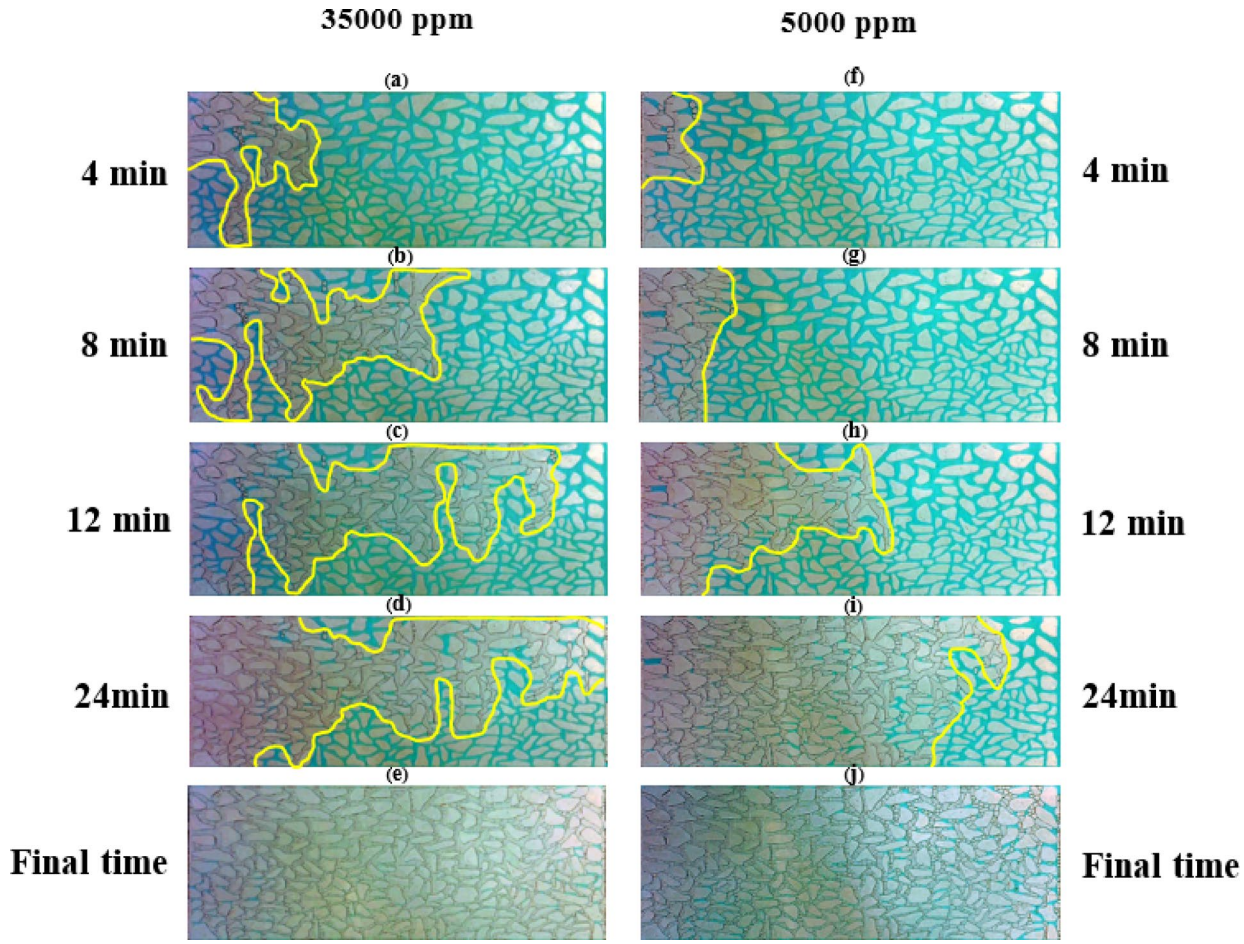

Fig. 4. Micromodel images of foam flow behavior at two different salinity levels (images "a to e" at 35,000 ppm salinity, and images "f to j" at 5,000 ppm salinity) at different time intervals.

the flow toward low permeable section. Thus, one can infer that the resulting conformance control in such heterogeneous media depends on the foam's initial stability. At high salinity condition, the low initial foam stability led to the formation of flow channel in the high-permeability layer, which limited fluid movement into the low-permeability layer. At lower salinity, greater foam stability enabled more uniform fluid distribution and improved displacement efficiency. Although the foam ultimately covered the entire porous medium in both cases, the quality of conformance at 35,000 ppm salinity was significantly lower. These findings suggest that high salinity poses a fundamental challenge for using foam in conformance control, as lower foam stability reduces its ability to block high-permeability zones and direct fluid toward low-permeability layers. Conversely, at 5,000 ppm salinity, foam demonstrated better performance in improving conformance and fluid displacement. These observations are consistent with the results of Bello et al.[44], who reported that increasing salinity reduced foam stability for anionic surfactants. In contrast, Le et al.[45] observed improved foam stability at high salinity when using a different, cationic foaming agent, indicating that the salinity effect is strongly surfactant-dependent and influenced by specific ion–surfactant interactions. To improve foam performance under high-salinity conditions, pre-injecting the surfactant solution can be considered as an effective strategy. This approach can enhance foam stability during the foam injection process by satisfying the surfactant coverage at the rock surface. According to adsorption principles, in the absence of surfactant preflush, part of surfactant molecules may adsorb onto the rock surface, thereby reducing its effective concentration in the aqueous phase for foam generation. Conversely, when the rock surface is pre-saturated with surfactant solution prior to foam injection, a larger fraction of the surfactant molecules remains active in foam generation, leading to improved foam stability. This hypothesis will be examined in the following section through complementary pore-scale insights.

Foam injection into SDS-saturated heterogeneous porous media

In this section, foam injection was performed into the micromodel pre-saturated with SDS solution. The images in Fig. 5 (a to e) showed foam injection at 35,000 ppm salinity into the surfactant-saturated environment. As the co-injection of gas and SDS solution began, the resulting foam front started advancing through the high-permeability layer (after 4 min). With continued injection, the SDS foam spread into both layers, establishing appropriate conformance (8 min). After 12 min, the leading edge of the foam front, which contained larger

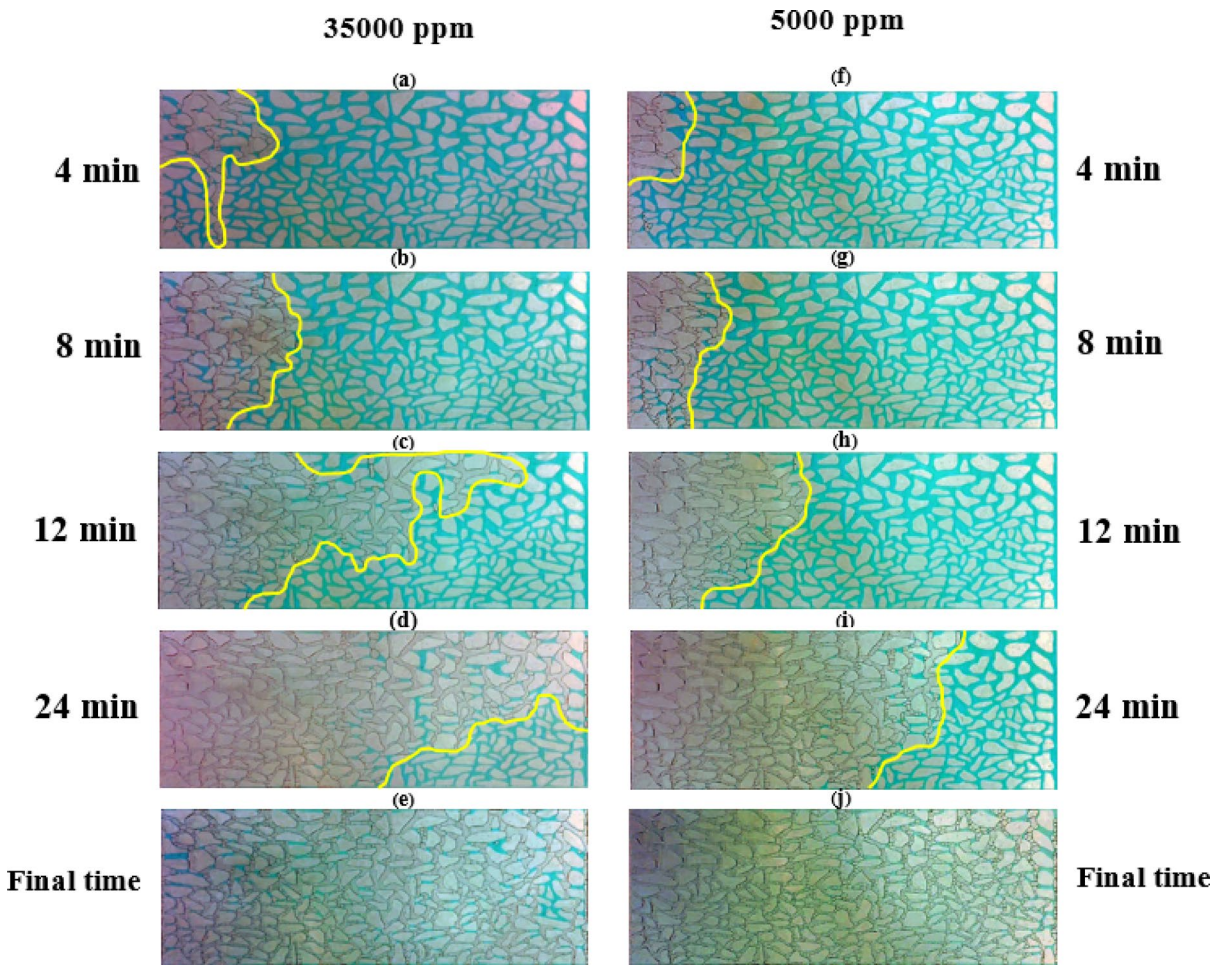

Fig. 5. Micromodel images of foam flow behavior with surfactant preflush at two different salinity levels (images "a to e" at 35,000 ppm salinity, images "f to j" at 5,000 ppm salinity) at different time intervals.

bubbles and was considered weaker foam, primarily advanced through the high-permeability layer, causing a reduction in conformance. Further foam injection till 24 min led to filling of high-permeability layer by foam and then diverting flow toward the low-permeability layer, ultimately covering the entire micromodel. Comparing the images in Fig. 4 (a to e) with those in Fig. 5 (a to e) demonstrated that the presence of surfactant preflush before foam injection resulted in more stable foam and improved conformance between low and high permeable layers. In contrast, without surfactant preflush, the foam flow behavior resembled that of weak foam or gas-like flow, and consequently weaker conformance between two layers. Similarly, in Fig. 5 (f to j), foam injection at 5,000 ppm salinity into the surfactant-saturated environment is shown. In this case, the foam initially advanced through the high-permeability layer (after 4 min) and then spread into both layers (at 8 min). As injection continued (till 12 and 24 min), a stable front formed, establishing good conformance in fluid movement, and eventually covered the entire environment. Foam injection in the presence of surfactant preflush increased the foam viscosity and thus more flow diversion toward the low-permeability layer, eventually resulting in good conformance between two layers. However, even in the absence of surfactant preflush and low salinity condition (Fig. 4, f to j), the SDS foam demonstrated satisfactory performance in controlling fluid movement and achieving conformance control. These results indicated that at such low salinity level SDS foam could provide a reasonable capability to control fluid flow the absence and presence of surfactant preflush.

Foam injection in the presence of waterflooded residual oil saturation

Figure 6 shows SDS foam injection in the presence of waterflooded residual oil at two different salinity levels. Initially, the micromodel was saturated with NaCl brine (either 35,000 or 5,000 ppm) and then flushed by oil (kerosene). Then, brine was injected at the flow rate of 0.002 mL/min until no oil was observed at the outlet. Then, by increasing the flow rate to 0.02 mL/min (representing the bump flow condition), brine was further injected into the micromodel to establish the residual oil saturation condition. Then, the SDS solution was injected as the preflush into the micromodel before foam injection. Figure 6 (a to e) shows foam injection at the salinity of 35,000 ppm. Upon initiation of gas and surfactant co-injection, the SDS foam was generated in the inlet section (foam chamber part) and then it advanced mainly through the high-permeability layer. When the SDS foam

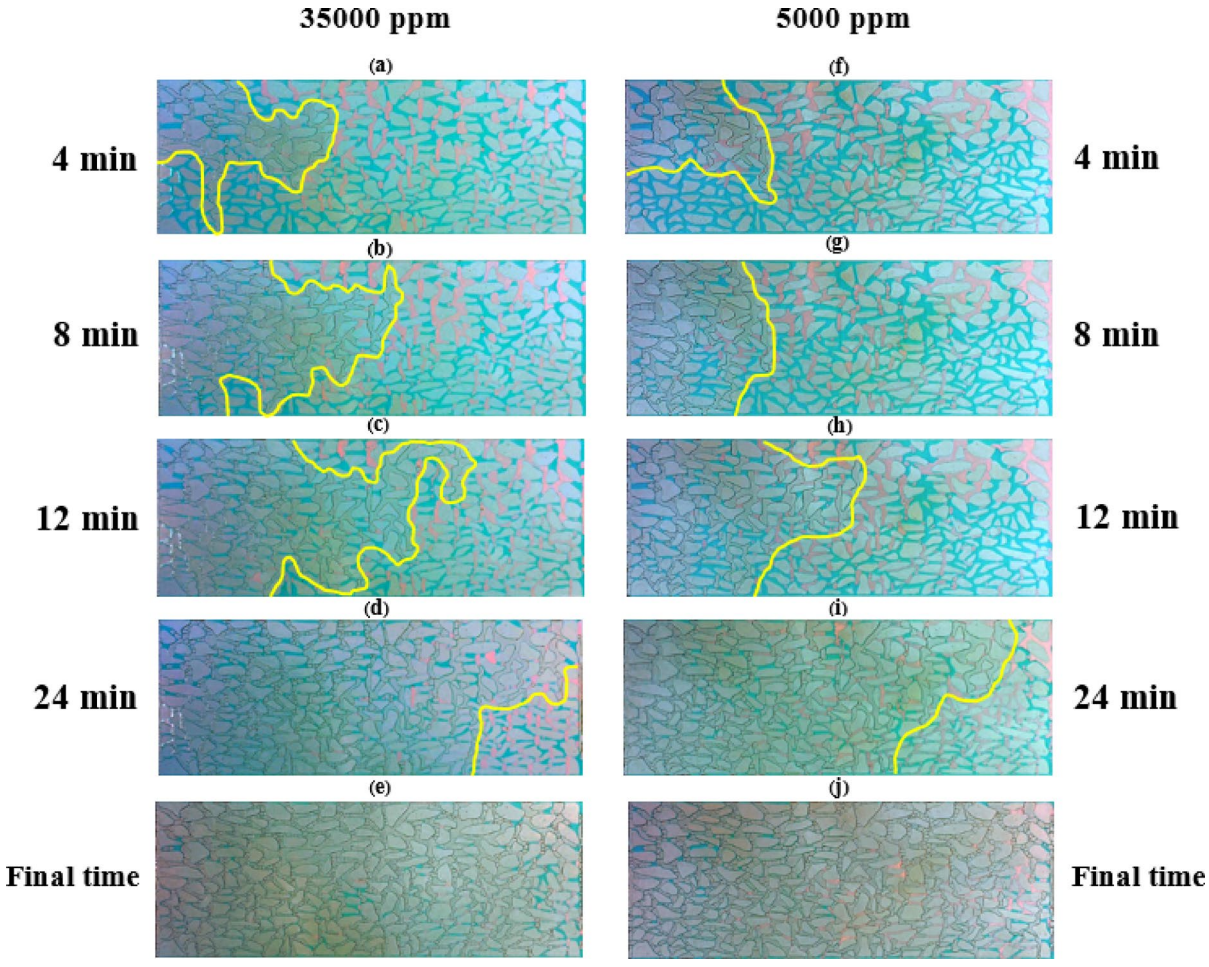

Fig. 6. Micromodel images of foam flow behavior in the presence of waterflooded residual oil at two different salinity levels (images "a to e" at 35,000 ppm salinity, images "f to j" at 5,000 ppm salinity) at different time intervals.

came in contact with the oil phase, foam films (lamellae) collapsed, forming weaker foam with larger bubbles, which leads to foam advancing primarily through the high-permeability layer (see images at 4 and 8 min). After displacing a portion of the waterflooded residual oil from the inlet region, more stable foam propagation was observed. However, the leading edge of the foam front, being more mobile than the rear, continued to advance through the high-permeability layer, resulting in weak conformance between two layers (see image at 12 min). As the stable foam front progressed further, more fluid diversion toward the low-permeability layer was observed. After 24 min, the conformance between two layers was significantly improved by the SDS foam, eventually the SDS foam covered the entire micromodel. Figure 6 (f to j) shows foam injection at 5,000 ppm salinity. At the start of foam injection, the SDS foam front propagates through the high-permeability layer (see image at 4 min). Although at this salinity the SDS foam became weakened upon contact with oil, it successfully maintained its advancement and established acceptable conformance control between two layers (see image after 8 min). Over time, the advancing foam front, which consists of larger bubbles, kept moving through the high-permeability layer (image at 12 and 24 min). Nevertheless, conformance control between two layers was maintained, and ultimately, the SDS foam occupied the micromodel.

Discussion

In this section, we examined the comparative analysis of SDS foam structure and its stability, as well as the interaction between foam and emulsions under different salinity conditions. By analyzing the pore-scale images, foam flow dynamics, and oil recovery performance, we aim to demonstrate how salinity affects foam flow dynamics and emulsion interactions. These findings provide a deeper understanding of the mechanisms underlying improved conformance control and oil displacement in a layered porous media.

Effect of salinity on the SDS foam structure under bulk and porous media conditions

Figure 7 shows microscopic images of the SDS foam generated under bulk conditions at two salinity levels (35,000 ppm and 5,000 ppm), along with the corresponding bubble number as a quantitative indicator of foamability. At high salinity, the foam exhibited a highly heterogeneous structure with a broad range of bubble sizes. This pronounced polydispersity stems from the destabilizing effect of high ionic strength on foam films. High salt concentrations compress the electrical double layer, reducing electrostatic repulsion and film elasticity, which accelerates bubble coalescence[46–49]. Furthermore, the broad size distribution can be attributed to enhanced Ostwald ripening, where gas diffuses from smaller, high-pressure bubbles to larger, low-pressure ones, promoting the growth of larger bubbles at the expense of smaller ones[50–52].

In contrast, at low salinity, the SDS foam exhibited a much more homogeneous structure with uniform bubble diameters. The reduced ionic strength preserves a strong electrostatic repulsion between surfactant-laden interfaces, effectively preventing coalescence and suppressing Ostwald ripening, thereby maintaining a consistent bubble size distribution[53,54]. Consequently, the bubble number at low salinity is higher and the size distribution is more uniform compared to the heterogeneous, lower-density foam formed at high salinity.

The structural trends observed in bulk were also replicated within the porous medium. Figure 8 shows pore-scale images of SDS foam at the two salinity levels, highlighting substantial differences in morphology and distribution. Under low-salinity conditions, the foam displayed a markedly higher bubble density with smaller diameters, leading to a homogeneous dispersion throughout the pore network. Conversely, high-salinity conditions resulted in a pronounced reduction in bubble number and the formation of larger bubbles, often several times the size of their low-salinity counterparts. This shift is attributed to the same destabilizing effects of

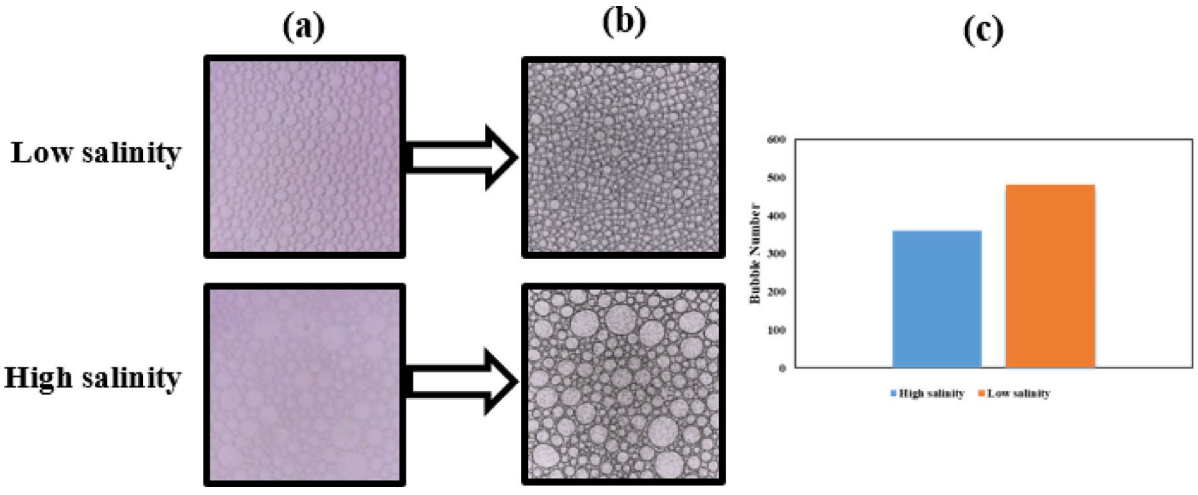

Fig. 7. Microscopic images of SDS bulk foam generated in the absence of oil at two salinity levels (5,000 ppm and 35,000 ppm). (**a**) Microscopic images captured at a fixed magnification, (**b**) Binary images describing SDS foam bubble structure, (**c**) Comparison of bubble number at two different salinity levels 5,000 ppm (right) and 35,000 ppm (left).

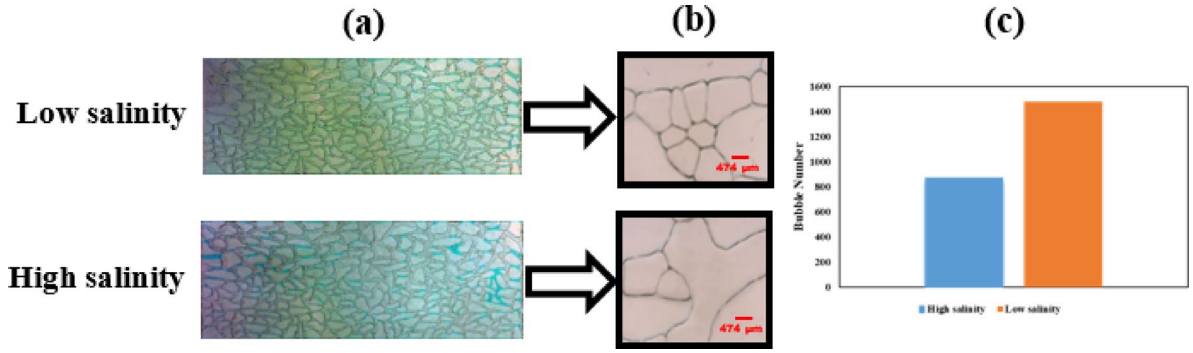

Fig. 8. (**a**) Microscopic images of the SDS foam through an oil-free porous media under two salinity levels (5,000 ppm and 35,000 ppm), (**b**) Pore-scale images of the SDS foam bubbles, (**c**) Comparison of bubble number at two different salinity levels 5,000 ppm (right) and 35,000 ppm (left).

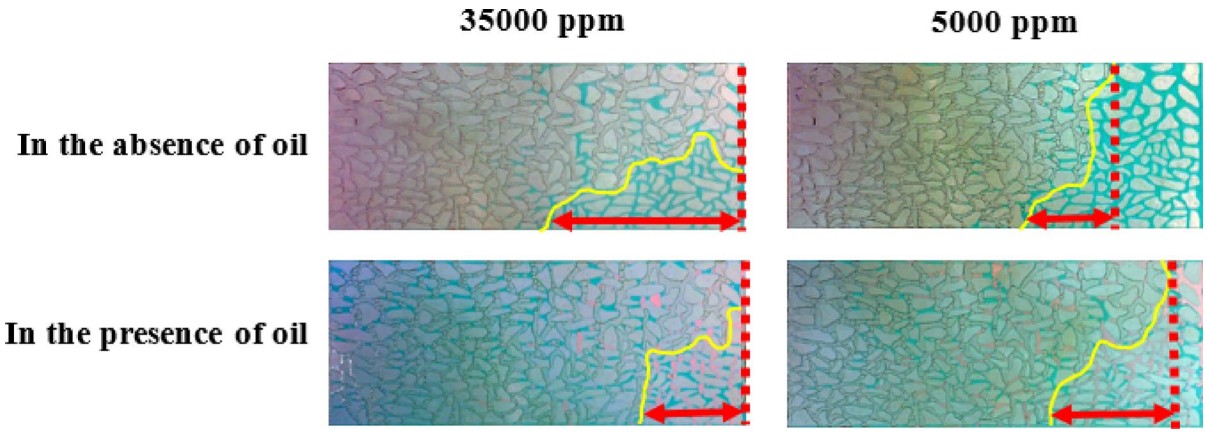

Fig. 9. Effect of salinity on foam and emulsion performance in conformance control at two salinity levels (35,000 ppm and 5,000 ppm) at a specific time, and in the presence and absence of waterflooded residual oil. The red arrow indicates the vertical distance between the foam fronts in the high-permeability (top) and low-permeability (bottom) layers, serving as a quantitative measure of interlayer conformance control. Shorter arrows reflect better conformance due to synchronized front advancement.

high ionic strength on liquid films, which promoted bubble coalescence and degraded the foam stability within the porous network[55–58].

Effect of salinity on foam and emulsion performance in conformance control

Figure 9 compares foam flow behavior at two salinity levels (35,000 ppm and 5,000 ppm) at a specific time, both in the presence and absence of waterflooded residual oil. As expected, foam stability decreases at high salinity (35,000 ppm) in the presence of residual oil due to their combined detrimental effects. However, the resulting flow behavior reveals a more complex picture. The advancing foam front, while less stable, initially moves through the high-permeability layer but later achieves significant conformance control with better interlayer coordination compared to the case without residual oil. In fact, in the absence of residual oil, conformance control is weaker and interlayer coordination decreases.

These counterintuitive results are governed by the formation and properties of oil-in-water emulsions, as shown in Fig. 10. The images indicate a clear difference in emulsion droplet size between the two salinity levels. At high salinity, larger emulsion droplets with a broader size distribution are formed. This occurs because the high concentration of salt ions compresses the electrical double layer, a phenomenon known as the ionic shielding effect. This shielding decreases the electrostatic repulsion among the anionic head-groups of SDS molecules, which diminishes their effective surface activity and reduces adsorption at the oil-water interface. Consequently, the surfactant's ability to lower interfacial tension is impaired, leading to the formation of larger, less stable droplets that are more prone to coalescence[17,59].

This emulsion behavior directly influences SDS foam flow dynamics in the porous medium. At high salinity, the larger emulsion droplets accumulate alongside the foam, temporarily blocking high-permeability pathways, particularly at pore throats. As these large droplets are forced through constrictions, they deform and generate an additional capillary resistance. This phenomenon, known as the Jamin effect, restricts flow through the high-permeability section and diverts the injected fluid toward the lower-permeability zone. This

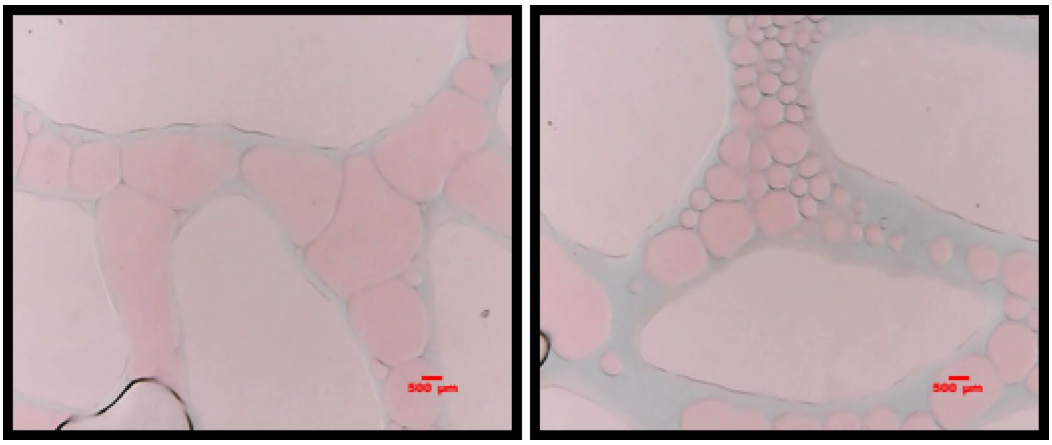

Fig. 10. In situ emulsion formation in the presence of the SDS surfactant at two salinity levels: 5,000 ppm (right) and 35,000 ppm (left). At the lower salinity, emulsion droplets are smaller, more uniform, and more stable (less prone to coalescence), whereas at the higher salinity, droplets are larger and less stable, with a greater tendency to coalesce.

mechanism is consistent with the pore-scale observations in Fig. 9, where enhanced conformance control is seen in the presence of residual oil. The process is dynamic; as foam injection continues and local pressure builds, the trapped emulsions deform and are released, after which the cycle of blockage and release can repeat. This recurring Jamin effect ensures sustained, long-term conformance control.

In contrast, the situation at low salinity (5,000 ppm) is different. The lower ion concentration results in a less compressed electrical double layer, increasing the repulsion among SDS head-groups and promoting more effective surfactant adsorption at the oil-water interface. This results in a greater reduction of interfacial tension and the formation of smaller, more uniform, and highly stable emulsion droplets, as shown in Fig. 10 (right image). These small droplets are less capable of blocking high-permeability zones and can easily pass through the wider pore throats. Therefore, a significant Jamin effect cannot occur in the high-permeability layer. Instead, the oil phase is transported as small, stable droplets through the high-permeability layer. Some of these droplets may enter and become trapped in the narrower pore throats of the low-permeability layer, potentially causing an unwanted Jamin effect that could impair flow in the low-permeability section.

Although both the SDS foam and the emulsions are more stable under low-salinity conditions, the system lacks the synergistic interaction required for effective diversion. The small emulsion droplets are ineffective at generating the necessary blockages in the high-permeability paths. Consequently, conformance control at low salinity reverts to being primarily governed by the foam itself, which proves less effective at achieving the targeted diversion seen in the high-salinity case.

The above results demonstrate that foam stability alone is an insufficient metric for evaluating the effectiveness of a diversion process. Fluid conformance, a key factor in improving displacement efficiency, is critically influenced by the size and stability of emulsion droplets. At high salinity, larger droplets and the dynamic Jamin effect work in concert with the foam to guide fluid flow and enhance conformance control. At low salinity, smaller, more stable droplets fail to block high-permeability pathways, leading to reduced overall conformance. Therefore, optimizing injection salinity is a key control parameter, as it governs not only foam stability but also the emulsion properties and their synergistic interaction with foam, ultimately determining the success of the combined foam-emulsion injection process for conformance control.

Effect of salinity on foam and emulsion performance in enhanced oil recovery

The interplay between foam and emulsions, governed by salinity, directly determines the effectiveness of enhanced oil recovery in layered porous media. Figure 11 illustrates foam flow behavior at two salinity levels in the presence of waterflooded residual oil at the end of foam injection stage. While foam in both cases diverts flow into the low-permeability layer and facilitates oil production, a key difference is evident: a greater amount of residual oil remains in the low-permeability layer at low salinity.

This lower recovery is a direct consequence of emulsion morphology. At low salinity, the formation of fine, highly stable emulsions leads to blockage within the narrow pore throats of the low-permeability layer. This unwanted Jamin effect reduces production efficiency and ultimately traps more oil. In contrast, the coarser, less stable emulsions generated at high salinity, prone to coalescence, promote the release and reconnection of the oil phase, facilitating its mobilization and resulting in a higher recovery rate.

Figure 12 quantifies this performance gap, showing a final recovery of 88.02% at high salinity compared to 78.81% at low salinity. This difference, a 9.20% point improvement (equivalent to an 11.7% relative increase), conclusively demonstrates the detrimental impact of stable fine emulsions in narrow pores and the greater displacement efficiency of coarser emulsions. Furthermore, the pore-throat blockage at low salinity risks significant operational challenges, including elevated pressure buildup and reduced injectivity. This indicates that salinity control is a critical parameter not only for maximizing recovery but also for ensuring long-term flow assurance and the effectiveness of subsequent displacement stages in layered reservoirs.

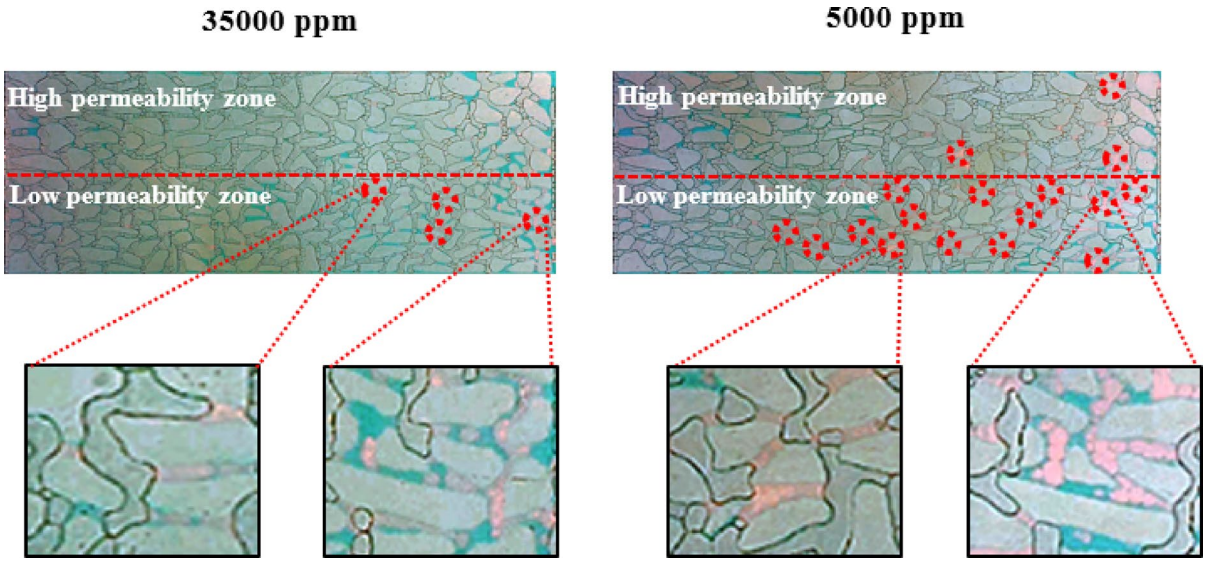

Fig. 11. Effect of salinity on foam and emulsion performance in the oil displacement at two salinity levels (35,000 ppm and 5,000 ppm) at the end of foam injection stage. The red circles indicate the Jamin effect at the pore-scale through layered micromodel.

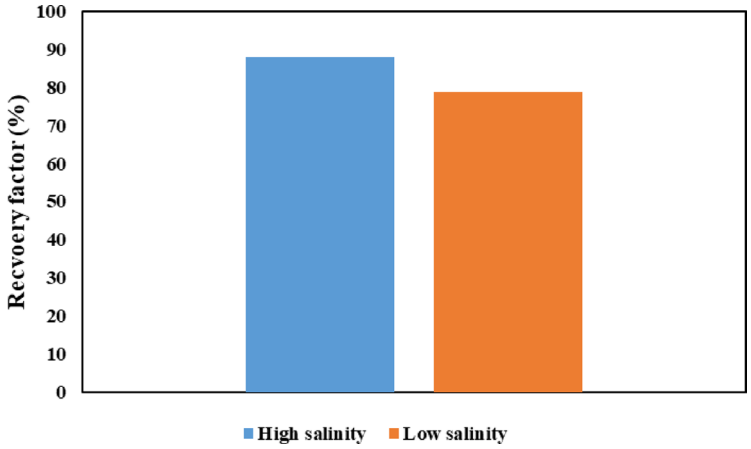

Fig. 12. Final oil recovery factor during foam injection at two salinity levels 5,000 ppm (right) and 35,000 ppm (left).

Conclusions

This pore-scale study demonstrated that the performance of foam in heterogeneous porous media is governed not merely by foam stability, but by the complex interplay between foam and in-situ generated emulsions, which is critically controlled by brine salinity. Using a layered micromodel and sodium dodecyl sulfate (SDS) surfactant, we visualized and mechanistically explained how salinity tailors this interaction to control flow diversion. The key findings are:

- Brine salinity directly controlled foam morphology: low salinity (5,000 ppm) generated a stable, fine-textured foam, while high salinity (35,000 ppm) produced a coarse, less stable foam due to the compression of the electrical double layer.
- The ultimate conformance control was governed not by foam stability alone, but by the complex interplay between the foam and in-situ generated emulsions.
- Under high-salinity conditions in the presence of waterflooded residual oil, the formation of large oil-in-water emulsion droplets created a dynamic Jamin effect. This mechanism caused effective temporary blockage in high-permeability pathways, forcing flow diversion into the low-permeability layer and improving sweep efficiency.
- In contrast, low-salinity conditions with oil generated smaller, more stable emulsions that failed to provide sufficient flow resistance in the high-permeability layer.

- Integrating all experiments revealed that salinity dictates a functional transition from a foam-viscosity-dominated regime at low salinity to an emulsion-diversion-dominated regime at high salinity. This transition stated that tuning salinity is essential for balancing these contributions to control overall diversion and displacement efficiency in layered systems.

Collectively, these findings establish that optimizing injection salinity is a crucial design parameter for foam processes. It provides a practical method for controlling both foam texture and emulsion droplet size, thereby activating the synergistic blocking mechanism needed for effective conformance control in heterogeneous systems. These insights are vital for designing efficient foam-assisted enhanced oil recovery and gas-based storage strategies in saline, heterogeneous reservoirs. Future work should focus on quantifying these effects at the core scale and developing predictive models that incorporate this newly identified foam-emulsion synergy.

Data availability

All data generated or analysed during this study are included in this published article.

Received: 13 August 2025; Accepted: 22 December 2025
Published online: 26 December 2025

References

1. Ding, B., Shi, L. & Dong, M. Conformance control in heterogeneous two-dimensional sandpacks by injection of oil-in-water emulsion: theory and experiments. *Fuel* **273**, 117751 (2020).
2. Kuehne, D. L., Ehman, D. I., Emanuel, A. S. & Magnani, C. F. Design and evaluation of a nitrogen-foam field trial. *J. Petrol. Technol.* **42**, 504–512 (1990).
3. Ahmadi, B., Molaei, A. H., Sahraei, E. & Mohammadi, A. H. Evaluation of competitive and synergistic effects of potential determining ions on interfacial tension reduction and wettability alteration in carbonate oil reservoirs. *Colloids Surf., A.* **713**, 136474 (2025).
4. Iravani, M., Simjoo, M. & Chahardowli, M. Exploring synergistic effects of graphene oxide and hydrolyzed polyacrylamide on rheology and thermal stability relevant to enhanced oil recovery. *Sci. Rep.* **15**, 27380 (2025).
5. Molaei, A., Iravani, M. & Simjoo, M. Enhanced oil recovery in a heterogeneous glass micro-model by application of low-concentration graphene oxide. *Pet. Sci. Technol.*, 1–19. (2025).
6. Iravani, M., Khalilnezhad, Z. & Khalilnezhad, A. A review on application of nanoparticles for EOR purposes: history and current challenges. *J. Petroleum Explor. Prod. Technol.* **13**, 959–994 (2023).
7. Larter, S., Adams, J., Gates, I., Bennett, B. & Huang, H. The origin, prediction and impact of oil viscosity heterogeneity on the production characteristics of Tar sand and heavy oil reservoirs. *J. Can. Pet. Technol.* **47** (2008).
8. Gotawala, D. R. & Gates, I. D. On the impact of permeability heterogeneity on SAGD steam chamber growth. *Nat. Resour. Res.* **19**, 151–164 (2010).
9. Alshehri, A. J., Wang, J., Kwak, H. T., AlSofi, A. M. & Gao, J. A study of gel-based conformance control within fractured carbonate cores using low-field nuclear-magnetic-resonance techniques. *SPE Reservoir Eval. Eng.* **22**, 1063–1074 (2019).
10. Abd, A. S., Zhang, N. & Abushaikha, A. S. Modeling the effects of capillary pressure with the presence of full tensor permeability and discrete fracture models using the mimetic finite difference method. *Transp. Porous Media*. **137**, 739–767 (2021).
11. Abd, A. S. & Abushaikha, A. S. Reactive transport in porous media: a review of recent mathematical efforts in modeling geochemical reactions in petroleum subsurface reservoirs. *SN Appl. Sci.* **3**, 401 (2021).
12. Sagbana, P. I. & Abushaikha, A. S. A comprehensive review of the chemical-based conformance control methods in oil reservoirs. *J. Petroleum Explor. Prod. Technol.* **11**, 2233–2257 (2021).
13. Torrealba, V. & Hoteit, H. Conformance improvement in oil reservoirs by use of microemulsions. *SPE Reservoir Eval. Eng.* **22**, 952–970 (2019).
14. Bai, B., Zhou, J. & Yin, M. A comprehensive review of polyacrylamide polymer gels for conformance control. *Pet. Explor. Dev.* **42**, 525–532 (2015).
15. Azari, M. & Soliman, M. Review of reservoir engineering aspects of conformance control technology. In *SPE Permian Basin Oil and Gas Recovery Conference* pp. SPE-35171-MS. (SPE, 1996).
16. Iravani, M., Simjoo, M. & Molaei, A. Synergistic effect of polymer and graphene oxide nanocomposite in heterogeneous layered porous media: a pore-scale EOR study. *J. Petroleum Explor. Prod. Technol.* **15**, 9 (2025).
17. Ahmadi, B., Sahraei, E. & Mohammadi, A. H. Investigation of the synergistic effects of SiO2 and Al2O3 nanoparticles with SDS and CTAB surfactants on the stability and improving phase behavior of water-oil emulsions. *Colloids Surf., A*. **705**, 135726 (2025).
18. Tang, K. et al. *Conformance Control and Improved Oil Recovery Mechanism of Branched Preformed Particle Gel in Fractured Reservoirs* (Utilizing Nuclear Magnetic Resonance Technology, Energy & Fuels, 2025).
19. Tang, J., Wei, B., Yang, M. & Rossen, W. R. Critical thresholds for CO2 foam generation in homogeneous porous media. *SPE J.* **30**, 439–454 (2025).
20. Molaei, A. H., Simjoo, M., Ebrahimi, M. & Roomi, A. Foam flow behavior for fluid diversion in heterogeneous, layered porous medium: microscale experimental study. *J. Petroleum Res.*, (2025).
21. Wang, Y. et al. *Analysis of Foam Mobility and Foam Texture in Heterogeneous Microfluidic* (Porous Media, Industrial & Engineering Chemistry Research, 2025).
22. Almajid, M. M. & Kovscek, A. R. Pore-level mechanics of foam generation and coalescence in the presence of oil. *Adv. Colloid Interface Sci.* **233**, 65–82 (2016).
23. Youssif, M. I., Sharma, K. V. & Piri, M. Hydrocarbon gas foam injection in fractured oil-wet carbonate samples: An experimental investigation of the effect of fracture-matrix permeability contrast on oil recovery. In *SPE Canadian Energy Technology Conference* pp. D012S004R001. (SPE, 2023).
24. Angarska, J. et al. Detection of the hydrophobic surface force in foam films by measurements of the critical thickness of the film rupture. *Langmuir* **20**, 1799–1806 (2004).
25. Du, D. X., Beni, A. N., Farajzadeh, R. & Zitha, P. L. Effect of water solubility on carbon dioxide foam flow in porous media: an X-ray computed tomography study. *Ind. Eng. Chem. Res.* **47**, 6298–6306 (2008).
26. Exerowa, D., Zacharieva, M., Cohen, R. & Platikanov, D. Dependence of the equilibrium thickness and double layer potential of foam films on the surfactant concentration. *Colloid Polym. Sci.* **257**, 1089–1098 (1979).
27. Qiao, X., Miller, R., Schneck, E. & Sun, K. Influence of salt addition on the surface and foaming properties of silk fibroin. *Colloids Surf., A*. **609**, 125621 (2021).
28. Izadi, M. & Kam, S. Investigating supercritical CO 2 foam propagation distance: conversion from strong foam to weak foam vs. Gravity segregation. *Transp. Porous Media*. **131**, 223–250 (2020).

29. Farajzadeh, R., Andrianov, A., Krastev, R., Rossen, W. & Hirasaki, G. Foam-oil interaction in porous media-Implications for foam-assisted enhanced oil recovery (SPE 154197). In *74th EAGE Conference and Exhibition incorporating EUROPEC 2012* pp. cp-293-00225 (European Association of Geoscientists & Engineers, 2012).
30. Rattanaudom, P., Shiau, B. J., Suriyapraphadilok, U. & Charoensaeng, A. Effect of pH on silica nanoparticle-stabilized foam for enhanced oil recovery using carboxylate-based extended surfactants. *J. Petrol. Sci. Eng.* **196**, 107729 (2021).
31. Obisesan, O., Ahmed, R. & Amani, M. The effect of salt on stability of aqueous foams. *Energies* **14**, 279 (2021).
32. Pandey, A., Sinha, A., Chaturvedi, K. R. & Sharma, T. Experimental investigation on effect of reservoir conditions on stability and rheology of carbon dioxide foams of nonionic surfactant and polymer: implications of carbon geo-storage. *Energy* **235**, 121445 (2021).
33. Simjoo, M., Rezaei, T., Andrianov, A. & Zitha, P. Foam stability in the presence of oil: effect of surfactant concentration and oil type. *Colloids Surf., A.* **438**, 148–158 (2013).
34. Saikia, T., Mejia, L., Sultan, A., Balhoff, M. & Hamad, J. A. Visualizing conformance control mechanisms in high-temperature reservoirs: a microfluidic analysis of Pickering emulsified gel systems. *Microfluid. Nanofluid.* **28**, 1–13 (2024).
35. Siavashi, J. et al. An insight into core flooding experiment via NMR imaging and numerical simulation. *Fuel* **318**, 123589 (2022).
36. Cuthiell, D., Sedgwick, G., Kissel, G. & Woolley, J. Steam corefloods with concurrent X-ray CT imaging. *J. Can. Pet. Technol.* **32** (1993).
37. Xu, K. et al. A 2.5-D glass micromodel for investigation of multi-phase flow in porous media. *Lab. Chip*. **17**, 640–646 (2017).
38. Patil, P. et al. CO2 foam field pilot test in sandstone reservoir: complete analysis of foam pilot response. In *SPE Improved Oil Recovery Conference?* pp. D041S017R002. (SPE, 2018).
39. Mirzaei, M. et al. CO2 foam pilot in a west texas field: Design, operation and results. In *SPE Improved Oil Recovery Conference?* pp. D011S007R002. (SPE, 2020).
40. Wilson, A. Field pilots show effectiveness of foams in Low-Porosity naturally fractured reservoir. *J. Petrol. Technol.* **67**, 120–122 (2015).
41. Wu, Z., Liu, H., Pang, Z., Wu, C. & Gao, M. Pore-scale experiment on blocking characteristics and EOR mechanisms of nitrogen foam for heavy oil: a 2D visualized study. *Energy Fuels*. **30**, 9106–9113 (2016).
42. Wang, Z. et al. Relationship between blocking performance and foam texture in porous media. *Geofluids* **2019**, 6315947 (2019).
43. Friedmann, F. & Jensen, J. *Some Parameters Influencing the Formation and Propagation of Foams in Porous Media* pp. SPE–15087 (SPE Western Regional Meeting, SPE, 1986).
44. Bello, A., Ivanova, A. & Cheremisin, A. Enhancing N2 and CO2 foam stability by surfactants and nanoparticles at high temperature and various salinities. *J. Petrol. Sci. Eng.* **215**, 110720 (2022).
45. Le, L., Ramanathan, R. & Nasr-El-Din, H. Evaluation of an ethoxylated amine surfactant for CO2-foam stability at high salinity conditions. In *Abu Dhabi International Petroleum Exhibition and Conference* pp. D031S094R003. (SPE, 2019).
46. Sharma, E. et al. Foam stabilization in salt solutions: the role of capillary drainage and Marangoni stresses. *J. Colloid Interface Sci.* **693**, 137535 (2025).
47. Nguyen, P. T. Stability and coalescence of bubbles in salt solutions in a bubble column and thin liquid films. (2017).
48. Chandran Suja, V., Kannan, A., Kubicka, B., Hadidi, A. & Fuller, G. Bubble coalescence at wormlike micellar solution–air interfaces. *Langmuir* **36**, 11836–11844 (2020).
49. Hunter, T. N., Pugh, R. J., Franks, G. V. & Jameson, G. J. The role of particles in stabilising foams and emulsions. *Adv. Colloid Interface Sci.* **137**, 57–81 (2008).
50. Cima, O. D., Rocha, C., Teixeira, A. & Wienke, B. Ostwald ripening for air bubbles and decompression illness: phenomenological aspects in diving. *arXiv* (2018).
51. Stevenson, P. Inter-bubble gas diffusion in liquid foam. *Curr. Opin. Colloid Interface Sci.* **15**, 374–381 (2010).
52. Lautze, N. C., Sisson, T. W., Mangan, M. T. & Grove, T. L. Segregating gas from melt: an experimental study of the Ostwald ripening of vapor bubbles in magmas. *Contrib. Miner. Petrol.* **161**, 331–347 (2011).
53. Huang, B., Nan, X., Fu, C. & Guo, T. Study of the bubble collapse mechanism and its influencing factors on stability under ultra-low surface tension. *Colloids Surf., A.* **618**, 126440 (2021).
54. Satpute, P. A. & Earthman, J. C. Hydroxyl ion stabilization of bulk nanobubbles resulting from microbubble shrinkage. *J. Colloid Interface Sci.* **584**, 449–455 (2021).
55. Xu, M. et al. Study on the strengthening mechanism of a mibc–peg mixed surfactant on foam stability. *ACS Omega.* **8**, 27429–27438 (2023).
56. Río-Arrillaga, R. D., García-Figueroa, A. A., López-Cervantes, J. L. & Albijanic, B. Gracia-Fadrique, hydrophobicity of Benzene-Based surfactants and its effect on bubble coalescence Inhibition. *Molecules* **29**, 5042 (2024).
57. Yu, K. et al. Foaming behavior of polymer-coated colloids: the need for Thick liquid films. *Langmuir* **33**, 6528–6539 (2017).
58. Vitasari, D., Cox, S., Grassia, P. & Rosario, R. Effect of surfactant redistribution on the flow and stability of foam films. *Proc. Royal Soc. A.* **476**, 20190637 (2020).
59. Ahmadi, B., Molaei, A. H., Sahraei, E. & Mohammadi, A. H. Exploring the effects of salinity and ionic composition on wettability alteration and interfacial properties in carbonate oil reservoirs. *Colloids Surf., A.* **713**, 136554 (2025).

Author contributions

A.H.M. conducted conceptualization, formal analysis, investigation, methodology, visualization, validation, writing—original draft, and writing—review & editing; M.S. contributed to conceptualization, validation, and writing—review & editing; M.Si. contributed to conceptualization, investigation, methodology, project administration, supervision, validation, and writing—review & editing. All authors reviewed and approved the final manuscript.

Declarations

Competing interests

The authors declare no competing interests.

Additional information

Correspondence and requests for materials should be addressed to M.S.

Reprints and permissions information is available at www.nature.com/reprints.

Publisher's note Springer Nature remains neutral with regard to jurisdictional claims in published maps and institutional affiliations.